Li, Y, Xu, J, Li, G, Wan, S, Batistic, O, Sun, M, Zhang, Y, Scott, R and Qi, B

 Protein S-acyl Transferase 15 is Involved in Seed Triacylglycerol Catabolism during Early Seedling Growth in Arabidopsis

http://researchonline.ljmu.ac.uk/id/eprint/11363/

Article

Protein S-acyl Transferase 15 is Involved in Seed Triacylglycerol Catabolism during Early Seedling Growth in Arabidopsis

Yaxiao Li[a][1,2], Jianfeng Xu[a][1,3], Gang Li[3], Si Wan[1], Oliver Batistic[4], Meihong Sun[5], Yuxing Zhang[3], Rod Scott[1], Baoxiu Qi[1,3,6]*

[1]Department of Biology and Biochemistry, University of Bath, Bath, BA2 7AY, UK

[2] Shanghai Center for Plant Stress Biology & National Key Laboratory of Plant Molecular Genetics, CAS Center for Excellence in Molecular Plant Sciences, Chinese Academy of Sciences, Shanghai 201602, China

[3]College of Horticulture, Hebei Agricultural University, Baoding, China

[4]Institut für Biologie und Biotechnologie der Pflanzen, Universität Münster, 48149 Muenster, Germany

[5]College of Horticulture, Shandong Agricultural University, Tai'an, China

[6]Pharmacy and Biomolecular Sciences, James Parsons Building, Byrom Street, Liverpool, L3 3AF, UK

Author for correspondence

Baoxiu Qi

Email: b.q@ljmu.ac.uk

[a]These authors contributed equally to this work

Highlight

Protein S-Acyl Transferase is involved β-oxidation of seed storage triacylglycerol in Arabidopsis which is required for normal post-germination growth of seedlings

Abstract

Seeds of Arabidopsis contain ~40% of triacylglycerol. It is converted to sugar to support post germination growth. We identified an Arabidopsis T-DNA knockout mutant that was sugar dependent during early seedling establishment. Our study showed that the β-oxidation process involved in catabolising the free fatty acids released from the seed triacylglycerol was impaired in this mutant. This mutant was confirmed to be transcriptional null for the Protein Acyl Transferase 15, AtPAT15 (At5g04270), one of the 24 protein acyl transferases in Arabidopsis. Although it is the shortest AtPAT15 contains the signature 'Asp-His-His-Cys cysteine rich domain' which is essential for the enzyme activity of this family of proteins. The function of AtPAT15 was validated because it rescued the growth defect of the yeast protein acyl transferase mutant *akr1* and it was also auto-acylated *in vitro*. Transient expression of AtPAT15 in Arabidopsis and tobacco localized AtPAT15 in the Golgi apparatus. Taken together, our data clearly demonstrated that AtPAT15 is involved in β-oxidation of triacylglycerol, revealing the importance of protein S-acylation in seed storage lipid breakdown during early seedling growth of Arabidopsis.

Introduction

Seed germination and seedling establishment are two important processes for spermatophytes before they acquire efficient photosynthesis to achieve self-sufficiency for further growth. While the mRNAs of genes required for seed germination have already been transcribed and accumulated during seed maturation, therefore, little energy is consumed, seedling establishment after post germination requires energy and carbon skeletons for DNA synthesis, new mRNA transcription, cell division, radicle elongation and other complex metabolic processes, hence relies on the complete breakdown of the major reserves in most seeds such as carbohydrates, proteins and lipids (Bewley, 1997; Rajjou *et al.*, 2004; Zhao *et al.*, 2018).

In Arabidopsis and other oilseed crops up to 40% of oil in the form of triacylglycerol (TAG) are stored in their fresh seeds. TAG is present in the cytosolic droplets that are enclosed by a phospholipid monolayer embedded with structural proteins (Eastmond, 2006; Siloto *et al.*, 2006). It has to be broken down completely to become accessible to support post-germination growth. TAG is first hydrolysed by lipases, releasing glycerol and free fatty acids (FFAs). Glycerol is then phosphorylated and converted to dihydroxyacetone phosphate (DHAP), while fatty acids are activated to acyl-CoAs at peroxisome, broken down to acetyl-CoAs via β-oxidation, and converted to organic acids such as oxaloacetate (OAA) via the glyoxylate cycle. DHAP and OAA enter gluconeogenesis and are converted to sugar which is used to fuel the early seedling growth (Eastmond and Graham, 2001; Canvin and Beevers, 1961; Cornah *et al.*, 2004; Theodoulou and Eastmond, 2012). Complete oxidation of TAG can produce more than twice the energy than the hydrolysis of protein and carbohydrate (Theodoulou and Eastmond, 2012).

Therefore, it is not surprising that many Arabidopsis mutants that are defective in early seedling establishment after germination are caused by the disruption of one or more genes

3

involved in the catabolism of their seed storage oil, and this defect can often be rescued by the addition of external sugar, such as sucrose (Graham, 2008). For example, the defective mutant of a lipase, Sugar Dependent 1 (SDP1), showed strong impairment in breaking down TAG, and the seedling of *sdp1* mutants grew much slower than wild type after germination. This defect was rescued by external sucrose supplement, indicating that TAG breakdown was essential in energy supply during early seedling growth and establishment (Eastmond, 2006). Similar phenotype was found in the loss-of-function mutant of *Peroxisomal ABC Transporter1* (*PXA1*). PXA1 is involved in the transportation of FFAs or fatty acyl-CoAs to peroxisomes (Zolman *et al.*, 2001). The conversion of FFAs to active fatty acyl-CoAs are catalyzed by two peroxisomal long-chain acyl-CoA synthetases (LACS6/7) and the *lacs6 lacs7* double mutant exhibited similar phenotype as the *pxa1* mutant in the reliance of sugar for seedling growth (Fulda *et al.*, 2004).

β-Oxidation is responsible for the breakdown of FFAs released from seed TAG thus disruption in β-oxidation results in stalled post-germination growth of seedling. For example, the first step of β-oxidation is mediated by the acyl-CoA oxidase (ACX) family proteins and seedlings of the double mutant *acx1acx2* failed to establish which is rescued by the addition of external sugar (Pinfield-Wells *et al.*, 2005). Multifunctional protein 2 (MFP2) and 3-ketoacyl-CoA thiolase 2 (KAT2) are involved in the second and final steps of β-oxidation process, therefore are also necessary for seedling establishment (Rylott *et al.*, 2006; Germain *et al.*, 2001). The isocitrate lyase (ICL) and malate synthase (MS), the key enzymes of glyoxylate cycle (Eastmond *et al.*, 2000; Cornah *et al.*, 2004), and phosphoenolpyruvate carboxykinase1 (PCK1), the catalytic enzyme for the first step of gluconeogenesis (Penfield *et al.*, 2004) are also proved to be essential for seedling establishment in Arabidopsis.

4

Protein S-acyl transferases (PATs) is a large family of enzymes that catalyse the S-acylation of proteins involved in signalling, trafficking and many other important functions in the cell (Resh, 2006; Li and Qi, 2017; Chen *et al*., 2018). S-acylation is a reversible post-translational lipid modification where a long chain fatty acid, commonly the 16-carbon palmitic acid, is attached to the cysteine residue(s) of a protein via a thioester bond. Many PATs have been characterised from yeast (Zhao *et al.*, 2002; Roth *et al.*, 2002; Valdez-Taubas and Pelham, 2005; Smotrys *et al.*, 2005; Lam *et al.*, 2006), mammals (Huang *et al.*, 2004; Fukata *et al.*, 2004; Swarthout *et al.*, 2005; Vetrivel *et al.*, 2009; Lakkaraju *et al.*, 2012; Yeste-Velasco *et al.*, 2015) and Arabidopsis (Hemsley *et al.*, 2005; Qi *et al.*, 2013; Li *et al.*, 2016). The common features of these PATs are the predicted 4-6 transmembrane domains (TMDs), and importantly, a conserved Asp-His-His-Cys cysteine rich domain (DHHC-CRD) which is proved to be the enzymatic catalytically active (Li and Qi, 2017; Chen *et al*., 2018).

In plants different numbers of DHHC-CRD containing proteins were reported in different plant species, from 6 in *Volvox carteri* to 52 in *Panicum virgatum* (Yuan *et al.*, 2013). Arabidopsis genome encodes 24 DHHC-PATs which were named as AtPAT1 to AtPAT24 (Hemsley *et al*, 2005; Batistic, 2012). From the characterisation of 4 AtPATs, AtPAT10 (Qi *et al.*, 2013), AtPAT13 (Lai *et al*, 2015), AtPAT14 (Li *et al.*, 2016) and AtPAT24 (Hemsley *et al.*, 2005), it is clear that AtPATs play important roles in plant growth, development, abiotic stress and senescence. For example, AtPAT24 (TIP1) loss-of-function mutants are semi-dwarf with very short root hairs (Hemsley *et al.*, 2005); *atpat10* was dwarf with much reduced fertility (Qi *et al*, 2013); the T-DNA knockout mutant plants of AtPAT14 exhibit an early leaf senescence phenotype which was enhanced by the introduction of a mutant allele of AtPAT13 (Lai *et al.*, 2015; Li *et al.*, 2016).

Here we report the functional characterization of another AtPAT, AtPAT15. Being the smallest PAT within the 24 PATs in Arabidopsis AtPAT15 is predicted to have 4 TMDs and a

conserved signature DHHC-CRD motif. It has PAT activity and localizes in the Golgi. The loss-of-function mutant of AtPAT15 exhibits multiple defects, such as delayed germination, failed seedling establishment, de-etiolation in the dark, reduced vegetative growth, and abnormal shoot apical meristem. We carried out in-depth analysis of the mutant seedling and found that the mutant failed to develop further after germination, importantly this defect was rescued by sucrose. Further studies proved that the breakdown of seed storage oil of the mutant is blocked and this is due to the ineffective β-oxidation, leading to the disruption for the FFAs released from TAG to convert to sugar. To our knowledge this is the first report to link protein S-acylation to seed lipid breakdown during early seedling growth, hence provide a new mechanism for lipid catabolism in Arabidopsis.

Materials and methods

Plant material and growth conditions

Wild-type Arabidopsis and the T-DNA insertion line SALK_006515 in the background of Columbia-0 were obtained from the Arabidopsis Biological Resources Center (ABRC, http://www.arabidopsis.org/abrc/). Seeds were surface sterilized, germinated and seedlings grown under long-day (LD) conditions as described previously (Qi *et al.*, 2013).

Identification of AtPAT15 T-DNA insertion mutant

PCR-based genotyping was carried out to isolate homozygous T-DNA insertion mutant plants from SALK_006515 line using primer pairs of LBb1/SALK006515RP and SALK006515LP/SALK006515RP (Table S1), respectively. PCR products amplified from the junction of the T-DNA insertion site were sequenced to confirm the exact T-DNA location in SALK_006515 according to Qi *et al* (2013).

6

In vitro pollen germination

The *in vitro* pollen germination assay was carried out according to Rodriguez-Enriquez et al (2013) with some adaptations. Briefly, mature pollen grains from WT and *pat15-1* were collected and placed on freshly prepared pollen growth media containing 18% sucrose, 0.8% agarose, 0.01% boric acid, 0.03% casein enzymatic hydrolysate, 1mM $CaCl_2$, 1mM $Ca(NO_3)_2$, 1mM KCl, 0.25mM spermidine, 0.01% myo-inositol and 0.01% ferric ammonium citrate. After incubation at 24^oC for 16 hours the growth of pollen tubes were observed and recorded under a dissecting microscope. The pollen germination rate was calculated as percentage of the number of germinated pollen grains out of total pollen grains placed on the media.

Complementation in yeast and Arabidopsis

The coding region of *AtPAT15* was amplified from the plasmid (in pGPTVII, Batistic, 2012) containing the 51-bp short version of *AtPAT15* by over-lapping PCR with primer pairs of PAT15F1/attB2PAT15R1, attB1PAT15F1/attB2PAT15R1 and attB1/attB2 (Table S1). The PCR product was recombined in the Gateway entry vector pDONR^{TM}/Zeo to create AtPAT15-pDONR (Invitrogen). To replace cysteine with serine in the DHHC motif PCR was performed with primer pairs of attB1/PAT15DHHC-S Rev and PAT15DHHC-S For/attB2 (Table S1) to generate two DNA fragments. The full length AtPAT15DHHC^{122}S was assembled by over-lapping PCR with primer pair of attB1/attB2 using these two DNA fragments as template and cloned in pDONR^{TM}/Zeo to generate AtPAT15DHHC^{122}S-pDONR (Qi et al, 2003). These two plasmids were re-combined into pYES-DEST52 (C-terminal V5 fusion) (Invitrogen) and pEarleyGate 103 (C-terminal GFP fusion) (Earley *et al.*, 2006) for expression in yeast and Arabidopsis, respectively. Transformation of yeast cells (wild-type and *akr1*), Arabidopsis plants and their subsequent growth were carried out as described

7

previously (Qi *et al.*, 2013; Li *et al.*, 2016).

Auto-acylation assay in yeast

The Acyl-RAC method was carried out on total proteins isolated from the transgenic *akr1* cells expressing AtPAT15-V5 and AtPAT15C^{122}S-V5 (Forrester *et al.* 2011). The proteins were separated via 10% SDS-PAGE and PAT15/PAT15C^{122}S were detected by Western blot with an anti-V5 antibody (mouse monoclonal antibody, KWBio, China) and ECL as described previously (Li *et al.*, 2016).

Subcellular localization of AtPAT15

Co-transformation and transient expression of the GFP tagged AtPAT15 and AtPAT15C^{122}S (in pEarleyGate103) and the mCherry tagged Golgi marker GNT1 (N-acetylglucosaminyltransferase I, At4g38240) in *Nicotiana benthamiana* leaves was performed as described previously (Batistič, 2012). For transient expression in Arabidopsis agrobacteria (strain GV3101) harbouring the above plasmids were grown for 16 hours. The cells were harvested, re-suspended in 10mM MES/KOH, 10 mM MgCl$_2$, 600 μM acetosyringone (pH 5.7) and incubated for three hours. Five-day old Arabidopsis seedlings that were grown on 1x MS were completely submerged in the agrobacteria solution (supplemented with 0.0002% Tween 20) and vacuum was applied with a water jet pump for 5 minutes. The vacuum was repeated twice more. After the agrobacteria were completely removed the seedlings were grown on fresh 1xMS media for further three days. The transiently expressed florescent proteins were observed by laser scanning confocal microscopy (Batistič, 2012).

8

RT-PCR and Real Time PCR

Total RNA was extracted with Trizol reagent (Invitrogen) according to the manufacturer's instructions. Oligo (dT)-primed cDNAs were synthesized from 1μg RNA using the First-Strand cDNA Synthesis Kit (Transgen, China). To detect transcripts in WT and *pat15-1* T-DNA homozygous insertion line, different primer pairs were used to amplify truncated transcripts spanning the T-DNA insertion site (F139+R981, F564+R910), up- (F139+R453) and down-stream (F813+R1045) of the T-DNA insertion site.

To detect expression of genes involved in lipid breakdown real time PCR was performed using the UltraSYBR PCR Mixture (With ROX, CWBIO, China) and the programme was run on a Stepone Plus real-time PCR system (Applied Biosystems). The relative transcript levels were calculated by the $2^{-\Delta\Delta t}$ method with the *AtEF-1α* gene (ACCESSION AAB07882) as an internal control (Livak *et al.*, 2001). At least three replicates were included in each experiment and this was repeated 3 times. The sequences of all primers used are listed in Supplemental Table S1&2.

Lipid analysis

The content of C20:1, a reliable TAG marker, was quantified from total fatty acids isolated from seedlings (Thazar-Poulot *et al.*, 2015). Briefly, 30 seeds or 40 five-day-old etiolated seedlings from each sample were collected, ground under liquid nitrogen and freeze-dried to constant weight. One mL of methylation solution (10% H_2SO_4 in methanol) and 10μl of 0.5mM heptadecanoic acid (as internal standard) were added. This was followed by heating at 85°C for 1 hour with occasional mixing. After cooling down to room temperature 1 mL of 1% NaCl and 0.5 mL of hexane were added and the content was mixed thoroughly by vortexing. After centrifugation the hexane layer containing the fatty acid methyl esters was removed and analyzed by gas-liquid chromatography-mass spectrophotometry (GC-MS) as

described previously (Browse *et al.*, 1986; Qi *et al.*, 2004).

To visualize the oil droplets in the hypocotyls 5-day-old dark-grown seedlings were immersed in 10μg/mL Nile Red solution for 5 minutes (Chen *et al.*, 2009). The stained hypocotyls were observed under excitation/emission of 488nm/583nm using a Nikon 90i Eclipse microscope.

GUS staining

To see the spatial and temporal expression of AtPAT15 promoter of *AtPAT15* (1,071bp upstream from the start codon of *AtPAT15*) was cloned with primers pPAT15attB1 and pPAT15attB2 (Table S1) and recombined to the Gateway plant expression vector pMDC162 containing the *GUS* reporter gene (Curtis and Grossniklaus, 2003). This was transferred in wild-type Arabidopsis Col-0 via the floral dipping method (Clough and Bent, 1998). Tissues from AtPAT15promoter:GUS transgenic Arabidopsis plants were stained in the staining buffer (100mM sodium phosphate buffer, pH7.0; 10mM EDTA; 0.1% triton X-100; 1mM $K_3Fe(CN)_6$; 2mM X-Gluc) at 37°C for 16 hours. There were cleared with 100% alcohol for 12 hours with several changes before imaging under a dissect microscope (Jefferson, 1987).

Assay for ß-oxidation

2, 4-Dichlorophenoxyacetic acid (2, 4-D), an herbicide that inhibits root growth, is synthesized via ß-oxidation from its precursor 4-(2, 4-dichlorophenoxy) butyric acid (2, 4-DB). Therefore, the conversion efficiency from 2,4-DB to 2,4-D is often used as an indication of the functionality of ß-oxidation. To see the effect of 2,4-D and 2,4-DB on root growth of seedlings, surface sterilized WT and *pat15-1* seeds were germinated and grown on ½ MS media with or without 0.5 μM 2,4-D or 2,4-DB for 7 days under LD conditions. The plates were then scanned and the root lengths measured with the ImageJ software. Similarly, the

effect of 1 μM of 2,4-D or 2,4-DB was observed and the hypocotyl lengths were measured of seedlings that were grown for 5 days in the dark (the plates were wrapped with double layered foil).

In vitro pollen germination

The *in vitro* pollen germination assay was carried out according to Rodriguez-Enriquez et al (2013) with some adaptations. Briefly, mature pollen grains from WT and *pat15-1* were collected and placed on freshly prepared pollen growth media containing 18% sucrose, 0.8% agarose, 0.01% boric acid, 0.03% casein enzymatic hydrolysate, 1mM $CaCl_2$, 1mM $Ca(NO_3)_2$, 1mM KCl, 0.25mM spermidine, 0.01% myo-inositol and 0.01% ferric ammonium citrate. After incubation at $24^\circ C$ for 16 hours the growth of pollen tubes were observed and recorded under a dissecting microscope. The pollen germination rate was calculated as percentage of the number of germinated pollen grains out of total pollen grains placed on the media.

Statistical analysis

One-way ANOVA and Tukey's HSD test were applied to compare three or more sets of data with Minitab, where different letters indicate significant differences between different treatments at $p<0.05$. To compare two sets of data the Student's *t*-test was used where * indicates significant difference with *p* values given in each figure legends. All the figures were drawn using Excel.

Results

Identification of AtPAT15 loss-of-function mutant

In order to understand the biological roles that AtPAT15 plays in the growth and development of Arabidopsis, we searched all the available mutant collection centres and identified an AtPAT15 T-DNA insertion line, SALK_006515 from ABRC. Through

sequencing the PCR product amplified using primers LBb1 and *AtPAT15* specific RP primer (Table S1) followed by sequence alignment with the *AtPAT15* genomic DNA sequence, the T-DNA insertion site was confirmed to be at nt1765 in the 6th exon of *AtPAT15*. RT-PCR using cDNA synthesized from RNA isolated from leaves of WT and the T-DNA insertion homozygous plants was carried out to determine the knockout status of this line. The result showed that no transcripts were detected with primers across the T-DNA insertion site (F139+R981, F564+R910). However, transcripts upstream (F139+R453) and downstream (F813+R1045) of the T-DNA insertion site were present. PCR products from all primer combinations were recovered from the WT (Fig. 1B), therefore confirming that SALK_006515 is a T-DNA knockout mutant for *AtPAT15*, hence, this line named as *atpat15-1* hereafter.

We next performed detailed phenotypic analysis of this line. As shown in Fig. 1 the rosette leaves of *pat15-1* were smaller, more rounded and crinkled compared to WT. The growth of *pat15-1* mutant plant during early developmental stages was very slow and the plant struggled to establish (Fig. 1D&E). However, as soon as the plant bolted this defect became less obvious and in fact, the mature mutant plant showed little difference compared to WT in terms of the number of branches, flower size and general appearance although it was slightly shorter than WT (Fig S1, Fig. S2A-F, Table 1). Because GUS expression level is higher in anthers (Fig. 2B, see below) we reasoned that *pat15-1* may have defect in pollen or/and pollen germination. However, the mutant pollen grains were germinated as well as WT where approximately 94% from both genotypes were germinated (Fig. S2C and G, and data not shown). Interestingly, the mutant produced larger seeds (26.3±0.79µg) that were about 20% heavier than WT seeds (21.2±0.79µg) (Fig. 1F&G) whilst the structure of the immature seeds at 3-day-after-pollination (DAP) was comparable between WT and the mutant (Fig. S2D&H).

12

AtPAT15 is ubiquitously expressed

To understand how AtPAT15 (gene locus: AT5G04270) functions in Arabidopsis, we monitored the transcript levels of *PAT15* by RT-PCR from total RNA isolated from seedlings and different tissues of mature WT Arabidopsis plants. We found that *PAT15* was expressed in samples with higher levels in young seedlings and rosette leaves (Fig. 2A). This is consistent with the expression pattern of *PAT15* analysed by online Arabidopsis eFP Browser (http://bbc.botany.utoronto.ca/efp/cgi-bin/efpWeb.cgi; Batistic, 2012). To further confirm this result, we observed the GUS distribution in transgenic Arabidopsis expressing PAT15promoter:GUS. Consistent with the RT-PCR result, GUS expression was detected in all tissues and seedlings where much higher levels were found in 7-day-old seedlings, rosette leaves and anthers (Fig. 2B). It is also noted that in 1- and 2-week-old seedlings, AtPAT15 expressed especially high in leaf veins (Fig. 2B-a&b).

AtPAT15 has a conserved DHHC-CRD and 4 trans-membrane domains

Previous studies showed that there are 24 DHHC-CRD proteins that may function as PATs in Arabidopsis (Hemsley *et al.*, 2005; Batistic, 2012). Among them, 3 have been identified to have PAT activity by *in vitro* and *in vivo* assays (Hemsley *et al.*, 2005; Qi *et al.*, 2013; Li *et al.* 2015). AtPAT15 was predicted to be the shorted PAT with only 3 TMDs and a luminal N-terminus (Batistic, 2012). However, the database of Arabidopsis, TAIR (The Arabidopsis Information Resource), has recently updated the information of *AtPAT15* where an extra 51 bps were added upstream of the previous cDNA sequence. Although it remains to be the shortest with the coding region being 816bp long, encoding a putative protein of 271 amino acids (molecular weight of approx. 30.6 kD) AtPAT15 now has 4 TMDs and the signature enzyme catalytic conserved DHHC-CRD resides in the cytosolic loop between the 2nd and 3rd

13

TMDs (Fig. S3B). This predicted structure of AtPAT15 resembles that of the majority of the PATs characterised so far. Other conserved domains/motifs in this family of proteins, such as the DPG and TTxE are also present (Montoro *et al.*, 2009; Batistic, 2012). The importance and function of these 2 domains are currently unknown.

AtPAT15 has PAT activity in yeast

Akr1 is one of the 7 yeast PATs and its knockout mutant *akr1* is sensitive to high temperature (37°C) and grows poorly under this restrictive temperature (Feng and Davis, 2000; Hemsley *et al.*, 2005). This feature is often used in complementation assays to show the functionality of a putative PAT. For example, the three functionally identified AtPATs, AtPAT24 (Hemsley *et al.*, 2005), AtPAT10 (Qi *et al.*, 2010) and AtPAT14 (Li *et al.*, 2016) of Arabidopsis can partially complement the growth defect of *akr1*, confirming them being PATs. To see if AtPAT15 also has this ability, we observed the phenotype of transgenic yeast cells harbouring AtPAT15 and its DHHC[122]S point-mutation variant. As shown in Fig 3A AtPAT15 largely rescued the growth defect of *akr1* because the phenotype of the cells appeared to be round (though larger) which was similar to the wild-type. However, the PAT15C[122]S expressing *akr1* yeast cells showed an elongated cell phenotype that resembles the mutant *akr1* cells.

To see if AtPAT15 is auto-acylated, we extracted total proteins from the above yeast cells and subjected to the acyl-RAC assay (Forrester et al., 2011). As shown in Fig 3B while AtPAT15 was captured on the beads and detected by Western blotting with anti-V5 antibody AtPAT15DHHC[122]S was not. This demonstrated that a fatty acid was attached to AtPAT15 via a liable thioester bound, i.e., it is auto-acylated whilst the mutant AtPAT15DHHC[122]S was not.

14

The above combined results demonstrate that AtPAT15 has PAT activity in yeast and this relies on the cysteine residue within the DHHC domain.

AtPAT15 is predominately localised in Golgi

Expression of GFP fusion of PAT15 in Arabidopsis and tobacco revealed that it is mainly localized in Golgi. This is further confirmed by co-localization with the mCherry tagged Golgi marker TGN1 (Fig 4; Fig S4). Similar localization profiles were observed with PAT15C^{122}S-GFP. Therefore, AtPAT15 is predominantly localized to the Golgi apparatus, indicating that the first TMD is required for correct localization of AtPAT15 as this is different from the previous observation made on the shorter 3 TMD containing AtPAT15 where a possible endoplasmic reticulum (ER) localization was indicated (Batistic, 2012).

Both WT DHH<u>C</u>-PAT15 and the point mutant DHH<u>S</u>-PAT15 can rescue the defect of pat15-1

To see if the altered phenotype of *pat15-1* is caused by the disruption of *AtPAT15* by T-DNA insertion we transformed *35S:PAT15* construct to *pat15-1* mutant. This showed that AtPAT15 can completely rescue the growth defect of *pat15-1* mutant since the transgenics appear identical to WT, demonstrating that the growth defect is indeed caused by disruption of AtPAT15 in the mutant (Fig. 5). However, surprisingly, when we introduced the AtPAT15 variant where the cysteine residue in the DHHC domain was changed to serine (*PAT15DHHC^{122}S*) the mutant plants can still rescue the growth defect of *pat15-1* (Fig. 5). The presence of T-DNA, its homozygosity and the presence of the transgene in PAT15 or PAT15DHHC^{122}S expressing lines were confirmed by PCR and sequencing (data not shown).

15

Therefore, the combined data demonstrate that the function of AtPAT15 does not rely on the Cys in the DHHC motif of AtPAT15 in Arabidopsis.

Post-germination growth of the pat15-1 mutant is sugar dependent

We routinely germinate and culture our seedling of Arabidopsis on sugar free ½ MS agar plate before putting them out in soil. For *pat15-1*, however, we noticed that although seed germination (appearance of radicle) was nearly normal but the early seedling growth of the mutant was defective where majority of the seedlings failed to develop further to produce true leaves. As shown in Fig. 6B followed by germination seedlings of the WT Arabidopsis continue to grow, leading to the fully expanded cotyledons, emergence of true leaves and elongated primary roots. However, seedlings of *pat15-1* mutant failed to grow, resulting in the arrest of cotyledon expansion and primary root elongation (Fig. 6B left). Interestingly, this was not due to failure in seed germination of *pat15-1* because at 92% majority of the mutant seeds were germinated after 72 hours compared to 98% of WT seeds did on the same sucrose-free media (Fig. 6A).

To see if sugar can help the mutant grow better we added 1% of sucrose to the ½ MS media. To our surprise the mutant seedlings could indeed develop and grow at a comparable rate as the WT seedlings (Fig. 6B right). Therefore, it is clear that the AtPAT15 loss-of-function mutant is sugar dependent during early seedling establishment.

AtPAT15 is involved in lipid catabolism during early seedling growth

In Arabidopsis, seed germination relies on the very limited sugar present in the seed. However, post-germination growth is supported by the breakdown of oil reserves

16

accumulated and stored in the seeds (Cornah *et al.*, 2004). Because seedlings of *pat15-1* failed to develop properly after germination without external sugar, we suspected that the lipid breakdown pathway during post germination growth may be defective in this mutant. Therefore, we measured the content of fatty acid C20:1 to monitor the efficiency of TAG breakdown in dark-grown *pat15-1* seedlings at the post-germination stage. C20:1 is a reliable marker routinely used to indicate the level of triacylglycerol (Thazar-Poulot *et al.*, 2015). *Sugar Dependent Protein1* loss-of-function mutant *sdp1* has a similar phenotype to *pat15-1* in post-germination growth due to a defect in lipid breakdown (Eastmond, 2006). Therefore, a direct comparison was made between WT, *pat15-1* and *sdp1*. First, we compared the C20:1 level in seeds of these three lines. However, we found no significant difference between these three lines, indicating that they all accumulated TAG normally during seed maturity (Fig. 7A). However, in 5-day-old seedlings of WT and *sdp1* 9.7% and 96.8% of C20:1 was detected, confirming the previous observation that most of the TAG in *sdp1* seedlings remains un-digested (Eastmond, 2006). Interestingly, C20:1 in *pat15-1* seedlings was 24.9%, which was significantly lower than WT but higher than *sdp1* (Fig. 7A), demonstrating that *pat15-1* mutant also has defect in lipid breakdown during post-germination growth although it is not as severe as *sdp1*.

Next, we analyzed the C20:1 content in 5-day-old etiolated seedlings that were grown on 1% sucrose containing media. This showed that only 22.2% in the WT was detected while 96.7% was found in *pat15-1* (Fig. 7A). Therefore, this clearly showed that sugar had inhibitory effect on lipid breakdown in both WT and *pat15-1* mutant seedlings, and this was particularly severe in the mutant where most of the seed storage lipid (~78%) remained intact.

To validate the above conclusion we observed the lipid droplets in Nile red stained hypocotyls of these seedlings. Consistent with the quantitative data the *pat15-1* hypocotyls were densely packed with oil droplets whilst there hardly any were observed in WT (Fig. 7B). Further, the mutant appeared to have even more oil droplets when grown on 1% sucrose containing media. This was in line with the higher C20:1 content (96.7%) in seedlings grown on sugar containing media compared to 24.9% of C20:1 found in those on sugar free media (Fig. 7A).

Taken together, the above results clearly demonstrated that AtPAT15 plays important roles during early seedling growth and this is mediated by its role in the regulation of seed storage lipid breakdown.

The expression of key genes during lipid breakdown is down-regulated in pat15-1

In order to determine which step(s) along the lipid breakdown pathway is defective in *pat15-1* we monitored the transcript levels of some key genes that are known to be involved in the different steps of this important process during early seedling growth. For this real time PCR was carried out by using cDNAs synthesized from total RNAs extracted from 10-day-old dark-grown WT and *pat15-1* seedlings. The genes tested included those encoding for 3-ketoacyl-CoA thiolase 2 (KAT2), Isocitrate lyase (ICL), malate synthase (MLS) and phosphoenolpyruvate carboxykinase1 (PCK1). The reason to choose these 4 genes is because their knockout mutant plants exhibited severe defect in lipid breakdown, leading to failed seedling establishment (Eastmond *et al.*, 2000; Germain*et al.*, 2001; Cornah *et al.*, 2004; Penfield *et al.*, 2004), which is similar to what was observed in *pat15-1* seedlings. As shown in Fig. 8 the expression level of *KAT2* in *pat15-1* was only 14.9% of that in WT while that of *ICL* and *MLS* in the mutant was even lower and accounted for 7.8% and 9.5% of those in WT respectively. At 36.6% the reduction in the transcript level of *PCK1* was not as severe as

18

KAT2, *ICL* and *MLS* but it was only 1/3 of that in WT. Therefore, the expression of all these 4 genes in *pat15-1* was much down regulated, indicating that the key genes for lipid breakdown in young seedlings of *pat15-1* were much less active than their counterparts in WT. This could lead to much less lipid breakdown hence less sugar synthesized to fuel the growth of the mutant seedlings. Therefore, these results further confirmed the regulatory role of AtPAT15 in lipid breakdown during the early seedling growth of Arabidopsis.

AtPAT15 affects lipid breakdown through β-oxidation process

Because the transcript of KAT2, the key enzyme involved in β-oxidation was down-regulated in the mutant we reasoned that β-oxidation is most likely to be defective in *pat15-1*. To prove this we carried out an assay to observe the root growth of WT and *pat15-1* seedlings that were cultured on 2, 4-D and 2, 4-DB. 2,4-D is a common herbicide which inhibits root growth in the light and hypocotyl elongation in the dark (Estelle and Somerville, 1987). Importantly, 2, 4-DB, the precursor of 2, 4-D can be converted to 2, 4-D through β-oxidation. Hence this process has been used previously to test β-oxidation efficiency in mutants that are defective in β-oxidation during lipid breakdown (Richmond and Bleecker, 1999; Eastmond *et al.*, 2000). Utilizing this method we first tested the inhibitory effect of 2, 4-D and found that the roots of both WT and *pat15-1* seedlings were indeed arrested when 0.5 μM of 2, 4-D was added in the media (Fig. 9A). Next, we added 0.5 μM of 2, 4-DB to the media and found that the roots of WT seedlings cannot elongate at all whilst those of *pat15-1* seedlings can still elongate although they were shorter compared to those grown on the control media lacking 2, 4-DB (Fig. 9B). Similar results were obtained when the hypocotyl lengths were measured from the dark-grown seedlings where the hypocotyls of *pat15-1* seedlings were much longer than those of WT when 0.5 μM 2, 4-DB was supplemented in the media (Figs. 9C & D).

19

From these experiments we can draw a conclusion that *pat15-1* seedlings produced much less herbicide 2, 4-D from its precursor 2, 4-DB and this is most likely due to the fact that β-oxidation was impaired in the mutant. Therefore, AtPAT15 plays positive roles in β-oxidation to breakdown the FFAs that are released from the seed storage TAG during early seedling growth.

Discussion

AtPAT15 has PAT activity

The ability of a putative PAT to completely or partially rescue the growth defect of the yeast PAT Akr1 knockout mutant is routinely used to validate its PAT activity of this newly identified PAT. Indeed, 4 yeast PATs, Akr1, Pfa3, Pfa4 and Pfa5 (Zhao *et al.*, 2002; Roth *et al.*, 2002; Valdez-Taubas and Pelham, 2005; Smotrys *et al.*, 2005; Lam *et al.*, 2006), 17 human PATs (DHHC1, 2, 3, 5–9, 10, 12, 14–18, 20 and 21, Huang *et al.*, 2004; Fukata *et al.*, 2004; Swarthout *et al.*, 2005; Vetrivel *et al.*, 2009; Lakkaraju *et al.*, 2012; Yeste-Velasco *et al.*, 2015) and 3 Arabidopsis PATs, AtPAT10, 14 and 24 (Hemsley *et al.*, 2005; Qi *et al.*, 2013; Li *et al.*, 2016) have been confirmed using this method. Therefore, we carried out similar assays by introducing *AtPAT15* into the *akr1* yeast cells. We found that the growth defect of *akr1* was partially restored as the cells were round although larger than the WT. However, the PAT15C[122]S transformed *akr1* yeast cells remained elongated that were similar to the *akr1* mutant cells (Fig. 3A). Furthermore, we also found that AtPAT15 is auto-acylated but AtPAT15C[122]S is not (Fig. 3B). This demonstrates that AtPAT15 has PAT activity in yeast and the cysteine in the DHHC motif is important for this function. However, in the Arabidopsis complementation study we discovered that both the WT- and DHHS-PAT15 can fully complement the growth defect of *pat15-1* (Fig. 5). This is different from other characterized

20

Arabidopsis PATs where the Cys in the DHHC was found essential for the enzyme activity because mutation to change Cys in the DHHC motifs to Aln or Ser of AtPAT10, 14 and 24 failed to rescue the phenotype of their respective knockout mutants (Hemsley *et al.*, 2005; Li *et al.*, 2015; Qi *et al.*, 2013).

Previous studies on the two yeast PATs Swf1 and Pfa4 also found that the mutants DHHR-Swf1 and DHHR- or DHHA-Pfa4 can still rescue the defects of *swf1* and *pfa4* (Montoro *et al.*, 2015). Therefore, it seems that the cysteine residue in the DHHC motif may not be the key functional residue in some PATs and AtPAT15 may fall into this category of PATs. As suggested these PATs may use other cysteine residues within the DHHC-CRD, or a different domain(s) to carry out their PAT activity, such as the PaCCT (Palmitoyltransferase Conserved C-Terminus) motif in Pfa3 and Swf1 (Montoro *et al.*, 2009). At least 70% of all PATs possess this domain and for AtPAT15 its PaCCT motif is found to be located between the 246-260th amino acids (Fig. S5). This PaCCT and/or indeed other cysteine residues within the DHHC-CRD may also play an important role in PAT activity of AtPAT15.

The lipid breakdown defect of pat15-1 is caused by defect in β-oxidation

For TAG in oilseed fully accessible to support early seedling growth it has to be firstly hydrolyzed by lipases. The free fatty acids released from TAG will undergo further breakdown by β-oxidation, glyoxylate cycle and gluconeogenesis to finally generate sugar. SDP1 encodes a triacylglycerol lipase, which initiates lipid reserves breakdown by removing the fatty acids from the glycerol backbone (Eastmond, 2006). The loss-of-function mutant *sdp1* has complete blockage in lipid breakdown, resulting in the failure in seedling establishment whilst its germination is unaffected (Eastmond, 2006). We found that seedlings of *sdp1* grown on sugar free media retained higher percentage of lipid storage than *pat15-1* (Fig. 7A). This indicates that *sdp1* failed to catabolize TAG to support seedling growth whilst

pat15-1 can still do so although to a much less extent than WT. This suggests that AtPAT15 functions differently from SDP1, therefore, it may not be involved in the SDP1/lipase mediated first step of TAG hydrolysis.

Further, we have observed that external carbon source can block lipid breakdown in *pat15-1* during early seedling growth. On the contrary, the lipid breakdown efficiency was enhanced by the addition of external sugar in the *icl* mutant which is defective in the glyoxylate cycle (Eastmond *et al.*, 2000). Therefore, it is unlikely that the lipid breakdown defect in *pat15-1* is caused by its involvement in the glyoxylate cycle, the last step of lipid breakdown that is mediated by ICL.

Therefore, AtPAT15-mediated lipid breakdown is distinctive from both SDP1 and ICL-mediated lipid breakdown during early seedling growth in Arabidopsis.

The fact that *pat15-1* is more resistant to 2,4-DB than WT demonstrates that less 2,4-D was produced in *pat15-1* compared to WT, i.e., the efficiency of β-oxidation in *pat15-1* is lower than that in WT seedlings (Fig. 9). This result provides evidence that the second step of lipid breakdown, the β-oxidation, was partially inhibited in *pat15-1*. Therefore, the sugar-dependent phenotype observed in early seedling growth of *pat15-1* is most likely caused by defect in β-oxidation during lipid catabolism. This is further supported by the very low transcript level of *KAT2* detected in the mutant seedlings as it is the key enzyme involved in β-oxidation (Fig. 8).

Beyond its role in the breakdown of storage lipid, β-oxidation has also been shown to be involved in the biosynthesis of fatty acid-based plant signalling molecules, such as jasmonic acid (JA), indole-3-acetic acid (IAA) and salicylic acid (SA), therefore, it regulates growth, development and stress responses in plants (Li *et al.*, 2005; Baker *et al.*, 2006; Nyathi and

22

Baker, 2006; Goepfert and Poirier, 2007; Zolman *et al.*, 2008). Consistent with this many mutants that have defective β-oxidation also exhibit altered growth and development patterns apart from the usual reduction of lipid breakdown during post-germination growth (Goepfert and Poirier, 2007). For example, the loss-of-function mutant of AIM1 (abnormal inflorescence meristem1), a multifunctional enzyme that also catalyzes the second step of β-oxidation during lipid catabolism showed severe defects in both vegetative and reproductive growth (Richmond and Bleecker, 1999). PXA1 (or PED3, PEROXISOME DEFECTIVE 3) supplies substrates for β-oxidation, and its loss-of-function mutant not only shows severe defects in seedling establishment but also strong abnormal phenotype in vegetative growth and seed size (Hayashi *et al.*, 2002; Mendiondo *et al.*, 2014). Acyl-coenzyme A oxidases which catalyze the first step of β-oxidation are also essential for JA production in peroxisomes. This exemplified by the fact that the wound-induced JA accumulation was abolished in the double mutant *acx1acx5*, leading to its enhanced sensitivity to chewing insects (Schilmiller *et al.*, 2007). Nevertheless, none of these mutants resemble the JA or IAA related mutants, indicating β-oxidation is also involved in other processes during plant growth and development in addition for pathways related to these phytohormones (Goepfert and Poirier, 2007). Similarly, *pat15-1* also shows multiple defects throughout its growth and development in addition to the early seedling stage (Fig. 1C and data not shown). The fact that sucrose could not rescue the growth defect in larger seedlings of *pat15-1* that were grown on sugar containing agar plates (Fig. 1C), or mature plants grown in soil (Fig. 1D) where sugar is synthesized and available by photosynthesis suggests that other cause(s) such as phytohormones may play roles in the altered phenotype.

The possible mechanism of the involvement of AtPAT15 in β-oxidation

23

It is clear that AtPAT15 is involved in the seed storage lipid breakdown process by regulating β-oxidation during early seedling establishment. The question is how this is carried out on a molecular level, i.e., what are the protein target(s) of AtPAT15 in this process? The most important role of a PAT is to catalyze the S-acylation of specific substrate protein(s). Therefore, we looked through the dataset of over 500 putative S-acylated proteins recently identified from Arabidopsis through proteomics (Hemsley et al., 2013). We found that ACX3, one of the key enzymes involved in β-oxidation of fatty acids are included in the dataset. ACX3 is one of the 6 acyl-CoA oxidase family proteins found in Arabidopsis that are involved in the first step of β-oxidation to breakdown FFAs released from TAG (Pinfield-Wells *et al.*, 2005). It is a medium-chain acyl-CoA oxidase, which is a cytoplasmic protein localized in peroxisome (Eastmond et al., 2000). AtPAT15 may target ACX3 to the peroxisome membrane via S-acylation where it carries out its function to convert the fatty acyl-CoA released from TAG to 2-trans-Enoyl-CoA, the product of the first step of ß-oxidation. If this is true, in the AtPAT15 loss-of-function mutant the lipid molecule attached to ACX3 by the action of AtPAT15 would be lost, causing the mis-localization hence dysfunction of ACX3 mediated lipid breakdown. This is supported by the fact that the *acx3* mutant showed similar resistance to 2, 4-DB as *pat15-1* (Rylott et al., 2003). Further experimentation will be carried out to validate this assumption.

In summary, we have characterized a DHHC-CRD containing protein in Arabidopsis, AtPAT15, which has similar structure as other identified PATs and has PAT activity. Importantly, the loss-of-function mutant of AtPAT15 has impaired function in hydrolyzing the seed storage lipid. This is because the β-oxidation for the breakdown of fatty acids released from triacylglycerol in its seed is defective. This leads to the failed seedling establishment of *pat15-1* without the supplementation of external sugar. Therefore, our data clearly demonstrated that AtPAT15 mediated protein S-acylation plays positive roles in seed storage

lipid catabolism during post-germination growth and early seedling establishment.

Acknowledgement

Supplementary data

Table S1. Sequences of primers used for cloning and genotyping
Table S2. Sequences of primers used for real time PCR
Fig. S1. Six week old soil grown plants of WT and *pat15-1*.
Fig. S2. Observation of fully opened flowers and *in vitro* pollen grain germination assays of WT and *pat15-1*.
A-D, WT; E-H, *pat15-1*. (A), (B), (E) and (F), fully opened flowers. (C)&(G), pollen germination assays. Pollen grains were germinated *in vitro* and observed according to Rodriguez-Enriquez et al (2013) (see Supplemental Method). (D)&(H), ovules at heart-stage (3 days after pollination). Arrows in C&G indicate pollen tubes. Scale bars in A&E=1mm, B&F=0.25mm and D&H=20μm.
Fig. S3. Prediction of protein topology of PAT15.
(A) The trans-membrane domains (TMDs) of PAT15 was predicted using TMHMM 2.0 software. The numbers on the horizontal axis represents the positions of the amino acids of PAT15 and the vertical axis the probability for each TMD at that position.
(B) Topological structure of PAT15 within the membrane drawn according to (A). The position of the DHHC-CRD was indicated.
Fig. S4. PAT15 is targeted to the Golgi in tobacco leaves.
AtPAT15-GFP or AtPAT15DHHS-GFP were co-expressed with AtGNT1-mCherry transiently in *N. benthamiana* leaves. Localization of the florescent proteins were observed by laser scanning confocal microscopy. Bars = 15 μm.
Fig. S5. Protein sequence alignment of some well characterized PATs by CLUSTAL Omega software. The DHHC-CRD (Asp-His-His-Cys Cystein rich domain, Green box) and PaCCT (Palmitoyltransferase Conserved C-Terminus, Yellow box) domains are highlighted. DPG (Asp-Pro-Gly) and TTxE (Thr-Thr-x-Glu) are also highlighted (both in purple boxes). Erf2, ACCESSION Q06551; Pfa3, ACCESSION NP_014073; Swf1, ACCESSION NP_010411; AtPAT24 (TIP1), ACCESSION NP_197535; HIP14 (DHHC17), ACCESSION AAH50324; AtPAT15, ACCESSION NP_196047

References

Baker A, Graham IA, Holdsworth M, Smith SM, Theodoulou FL. 2006. Chewing the fat: β-oxidation in signalling and development. Trends in plant science **11**, 124-132.

Batistič O. 2012. Genomics and Localization of the Arabidopsis DHHC-Cysteine-Rich Domain S-Acyltransferase Protein Family. Plant Physiology **160**, 1597-1612.

Bewley JD. 1997. Seed germination and dormancy. The plant cell **9**, 1055.

Bewley JD, Black M. 1994. Seeds: Springer.

Borek S, Nuc K. 2011. Sucrose controls storage lipid breakdown on gene expression level in germinating yellow lupine (Lupinus luteus L.) seeds. Journal of plant physiology **168**, 1795-1803.

Browse J, McCourt PJ, Somerville CR. 1986. Fatty acid composition of leaf lipids determined after combined digestion and fatty acid methyl ester formation from fresh tissue. Analytical Biochemistry **152**, 141-145.

Canvin DT, Beevers H. 1961. Sucrose synthesis from acetate in the germinating castor bean: kinetics and pathway. Journal of Biological Chemistry **236**, 988-995.

Chen W, Zhang C, Song L, Sommerfeld M, Hu Q. 2009. A high throughput Nile red method for quantitative measurement of neutral lipids in microalgae. Journal of Microbiological Methods **77**, 41-47.

Chen B, Sun Y, Niu J, Jarugumilli GK, Wu X. 2018. Protein lipidation in cell signalling and diseases: function, regulation and theruputic opportunities. Cell Chemical Biology 25, 817-831

Clough SJ, Bent AF. 1998. Floral dip: a simplified method for *Agrobacterium*-mediated transformation of *Arabidopsis thaliana*. Plant Journal **16**, 735–743

Cornah JE, Germain V, Ward JL, Beale MH, Smith SM. 2004. Lipid Utilization, Gluconeogenesis, and Seedling Growth in Arabidopsis Mutants Lacking the Glyoxylate Cycle Enzyme Malate Synthase. Journal of Biological Chemistry **279**, 42916-42923.

Cutler S, Ghassemian M, Bonetta D, Cooney S, McCourt P. 1996. A protein farnesyl transferase involved in abscisic acid signal transduction in Arabidopsis. Science **273**, 1239.

Eastmond PJ. 2006. SUGAR-DEPENDENT1 Encodes a Patatin Domain Triacylglycerol Lipase That Initiates Storage Oil Breakdown in Germinating Arabidopsis Seeds. The Plant Cell **18**, 665-675.

Eastmond PJ. 2007. MONODEHYROASCORBATE REDUCTASE4 is required for seed storage oil hydrolysis and postgerminative growth in Arabidopsis. *The Plant Cell* **19**, 1376-1387.

Eastmond PJ, Germain V, Lange PR, Bryce JH, Smith SM, Graham IA. 2000. Postgerminative growth and lipid catabolism in oilseeds lacking the glyoxylate cycle. Proceedings of the National Academy of Sciences **97**, 5669-5674.

Eastmond PJ, Graham IA. 2001. Re-examining the role of the glyoxylate cycle in oilseeds. Trends in plant science **6**, 72-78.

Feng Y, Davis NG. 2000. Akr1p and the type I casein kinases act prior to the ubiquitination step of yeast endocytosis: Akr1p is required for kinase localization to the plasma membrane. Molecular and cellular biology **20**, 5350-5359.

Forrester MT, Hess DT, Thompson JW, Hultman R, Moseley MA, Stamler JS, Casey PJ 2011. Site-specific analysis of protein S-acylation by resin-assisted capture. Journal of lipid research. **52,** 393-398.

Frey A, Audran C, Marin E, Sotta B, Marion-Poll A. 1999. Engineering seed dormancy by the modification of zeaxanthin epoxidase gene expression. Plant molecular biology **39**, 1267-1274.

Fukata M, Fukata Y, Adesnik H, Nicoll RA, Bredt DS. 2004. Identification of PSD-95 palmitoylating enzymes. *Neuron* **44**, 987-996.

Fulda M, Schnurr J, Abbadi A, Heinz E. 2004. Peroxisomal Acyl-CoA synthetase activity is essential for seedling development in Arabidopsis thaliana. The Plant Cell **16**, 394-405.

Germain V, Rylott EL, Larson TR, Sherson SM, Bechtold N, Carde J-P, Bryce JH, Graham IA, Smith SM. 2001. Requirement for 3-ketoacyl-CoA thiolase-2 in peroxisome development, fatty acid β-oxidation and breakdown of triacylglycerol in lipid bodies of Arabidopsis seedlings. The Plant Journal **28**, 1-12.

Goepfert S, Poirier Y. 2007. β-Oxidation in fatty acid degradation and beyond. Current opinion in plant biology **10**, 245-251.

Gonzalez MA, Quiroga R, Maccioni H, Valdez TJ. 2009. A novel motif at the C-terminus of palmitoyltransferases is essential for Swf1 and Pfa3 function in vivo. *Biochem. J* **419**, 301-308.

Graham IA. 2008. Seed storage oil mobilization. *Annual Review of Plant Biology* **59**, 115-142.

Grappin P, Bouinot D, Sotta B, Miginiac E, Jullien M. 2000. Control of seed dormancy in Nicotiana plumbaginifolia: post-imbition abscisic acid synthesis imposes dormancy maintenance. Planta **210**, 279-285.

Hayashi M, Nito K, Takei-Hoshi R, Yagi M, Kondo M, Suenaga A, Yamaya T, Nishimura M. 2002. Ped3p is a peroxisomal ATP-binding cassette transporter that might supply substrates for fatty acid β-oxidation. Plant and Cell Physiology **43**, 1-11.

Hemsley PA, Grierson CS. 2011. The ankyrin repeats and DHHC S-acyl transferase domain of AKR1 act independently to regulate switching from vegetative to mating states in yeast. PloS one **6**, e28799.

Hemsley PA, Kemp AC, Grierson CS. 2005. The TIP GROWTH DEFECTIVE1 S-acyl transferase regulates plant cell growth in Arabidopsis. Plant Cell **17**, 2554-2563.

Huang K, Yanai A, Kang R, Arstikaitis P, Singaraja RR, Metzler M, Mullard A, Haigh B, Gauthier-Campbell C, Gutekunst C-A. 2004. Huntingtin-interacting protein HIP14 is a palmitoyl transferase involved in palmitoylation and trafficking of multiple neuronal proteins. Neuron **44**, 977-986.

Jacobsen SE, Olszewski NE. 1993. Mutations at the SPINDLY locus of Arabidopsis alter gibberellin signal transduction. The Plant Cell **5**, 887-896.

Jefferson RA. 1987. Assaying chimeric genes in plants: the GUS gene fusion system. Plant molecular biology reporter **5**, 387-405.

Koornneef M, Bentsink L, Hilhorst H. 2002. Seed dormancy and germination. Current opinion in plant biology **5**, 33-36.

Koornneef M, Van der Veen J. 1980. Induction and analysis of gibberellin sensitive mutants in Arabidopsis thaliana (L.) Heynh. Theoretical and Applied Genetics **58**, 257-263.

Lai J, Yu B, Cao Z, Chen Y, Wu Q, Huang J, Yang C. 2015. Two homologous protein S-acyltransferases, PAT13 and PAT14, cooperatively regulate leaf senescence in Arabidopsis. Journal of Experimental Botany **66**, 6345-6353.

Lakkaraju AK, Abrami L, Lemmin T, Blaskovic S, Kunz B, Kihara A, Dal Peraro M, van der Goot FG. 2012. Palmitoylated calnexin is a key component of the ribosome–translocon complex. The EMBO journal **31**, 1823-1835.

Lam KK, Davey M, Sun B, Roth AF, Davis NG, Conibear E. 2006. Palmitoylation by the DHHC protein Pfa4 regulates the ER exit of Chs3. The Journal of cell biology **174**, 19-25.

Lemieux B, Miquel M, Somerville C, Browse J. 1990. Mutants of Arabidopsis with alterations in seed lipid fatty acid composition. Theoretical and Applied Genetics **80**, 234-240.

Li C, Schilmiller AL, Liu G, Lee GI, Jayanty S, Sageman C, Vrebalov J, Giovannoni JJ, Yagi K, Kobayashi Y. 2005. Role of β-oxidation in jasmonate biosynthesis and systemic wound signaling in tomato. The Plant Cell **17**, 971-986.

Li Y, Qi B. 2017. Progress toward understanding protein S-acylation: prospective in plants. Frontiers in Plant Science **8(346)**, 1-20

Li Y, Scott RJ, Doughty J, Grant M, Qi B. 2016. Protein S-Acyltransferase 14: a specific role for palmitoylation in leaf senescence in Arabidopsis. *Plant physiology*, pp. 00448.02015.

Mönke G, Seifert M, Keilwagen J, Mohr M, Grosse I, Hähnel U, Junker A, Weisshaar B, Conrad U, Bäumlein H. 2012. Toward the identification and regulation of the Arabidopsis thaliana ABI3 regulon. Nucleic acids research **40**, 8240-8254.

Martínez-Andújar C, Ordiz MI, Huang Z, Nonogaki M, Beachy RN, Nonogaki H. 2011. Induction of 9-cis-epoxycarotenoid dioxygenase in Arabidopsis thaliana seeds enhances seed dormancy. Proceedings of the National Academy of Sciences **108**, 17225-17229.

Mendiondo GM, Medhurst A, van Roermund CW, Zhang X, Devonshire J, Scholefield D, Fernández J, Axcell B, Ramsay L, Waterham HR. 2014. Barley has two peroxisomal ABC transporters with multiple functions in β-oxidation. Journal of experimental botany **65**, 4833-4847.

Montoro AG, Quiroga R, Maccioni HJ, Taubas JV. 2009. A novel motif at the C-terminus of palmitoyltransferases is essential for Swf1 and Pfa3 function in vivo. Biochemical Journal **419**, 301-308.

Montoro AG, Ramirez SC, Quiroga R, Taubas JV. 2011. Specificity of transmembrane protein palmitoylation in yeast. PLoS One **6**, e16969.

Nyathi Y, Baker A. 2006. Plant peroxisomes as a source of signalling molecules. Biochimica et Biophysica Acta (BBA)-Molecular Cell Research **1763**, 1478-1495.

Ogawa M, Hanada A, Yamauchi Y, Kuwahara A, Kamiya Y, Yamaguchi S. 2003. Gibberellin biosynthesis and response during Arabidopsis seed germination. The Plant Cell **15**, 1591-1604.

Ohno Y, Kashio A, Ogata R, Ishitomi A, Yamazaki Y, Kihara A. 2012. Analysis of substrate specificity of human DHHC protein acyltransferases using a yeast expression system. Molecular biology of the cell **23**, 4543-4551.

Penfield S, Rylott EL, Gilday AD, Graham S, Larson TR, Graham IA. 2004. Reserve mobilization in the Arabidopsis endosperm fuels hypocotyl elongation in the dark, is independent of abscisic acid, and requires PHOSPHOENOLPYRUVATE CARBOXYKINASE1. The Plant Cell **16**, 2705-2718.

Pinfield- Wells H, Rylott EL, Gilday AD, Graham S, Job K, Larson TR, Graham IA. 2005. Sucrose rescues seedling establishment but not germination of Arabidopsis mutants disrupted in peroxisomal fatty acid catabolism. The Plant Journal **43**, 861-872.

Pryciak PM, Hartwell LH. 1996. AKR1 encodes a candidate effector of the G beta gamma complex in the Saccharomyces cerevisiae pheromone response pathway and contributes to control of both cell shape and signal transduction. Molecular and Cellular Biology **16**, 2614-2626.

Qi B, Doughty J, Hooley R. 2013. A Golgi and tonoplast localized S-acyl transferase is involved in cell expansion, cell division, vascular patterning and fertility in Arabidopsis. New Phytologist **200**, 444-456.

Qi B, Fraser T, Mugford S, Dobson G, Sayanova O, Butler J, Napier JA, Stobart AK, Lazarus CM. 2004. Production of very long chain polyunsaturated omega-3 and omega-6 fatty acids in plants. Nature Biotechology **22**, 739-745.

Quettier A-L, Eastmond PJ. 2009. Storage oil hydrolysis during early seedling growth. Plant Physiology and Biochemistry **47**, 485-490.

Rajjou L, Gallardo K, Debeaujon I, Vandekerckhove J, Job C, Job D. 2004. The effect of α-amanitin on the Arabidopsis seed proteome highlights the distinct roles of stored and neosynthesized mRNAs during germination. Plant Physiology **134**, 1598-1613.

Rodriguez-Enriquez M J, Mehdi S, Dickinson HG, Grant-Downton RT 2013**.** A novel method for efficient in vitro germination and tube growth of Arabidopsis thaliana pollen. New Phytolologist **197(2): 668-679.Resh MD**. 2006. Palmitoylation of ligands, receptors, and intracellular signaling molecules. Science Signaling **2006**, re14-re14.

Richmond TA, Bleecker AB. 1999. A defect in β-oxidation causes abnormal inflorescence development in Arabidopsis. The Plant Cell **11**, 1911-1923.

Rodriguez-Enriquez MJ, Mehdi S, Dickinson HG and Grant-Downton RT. 2013. A novel method for efficient in vitro germination and tube growth of Arabidopsis thaliana pollen. New Phytologist **197**, 668-679.

Roth AF, Feng Y, Chen L, Davis NG. 2002. The yeast DHHC cysteine-rich domain protein Akr1p is a palmitoyl transferase. The Journal of cell biology **159**, 23-28.

Roth AF, Wan J, Bailey AO, Sun B, Kuchar JA, Green WN, Phinney BS, Yates JR, Davis NG. 2006. Global analysis of protein palmitoylation in yeast. Cell **125**, 1003-1013.

Rylott EL, Rogers CA, Gilday AD, Edgell T, Larson TR, Graham IA. 2003. Arabidopsis mutants in short- and medium-chain acyl-CoA oxidase activities accumulate acyl-CoAs and reveal that fatty acid β-oxidation is essential for embryo development. Journal of Biological Chemistry **278**, 21370–21377

Rylott EL, Eastmond PJ, Gilday AD, Slocombe SP, Larson TR, Baker A, Graham IA. 2006. The Arabidopsis thaliana multifunctional protein gene (MFP2) of peroxisomal β- oxidation is essential for seedling establishment. The Plant Journal **45**, 930-941.

Schilmiller AL, Koo AJ, Howe GA. 2007. Functional diversification of acyl-coenzyme A oxidases in jasmonic acid biosynthesis and action. Plant Physiology **143**, 812-824.

Siloto RM, Findlay K, Lopez-Villalobos A, Yeung EC, Nykiforuk CL, Moloney MM. 2006. The accumulation of oleosins determines the size of seed oilbodies in Arabidopsis. The Plant Cell **18**, 1961-1974.

Smeekens S, Ma J, Hanson J, Rolland F. 2010. Sugar signals and molecular networks controlling plant growth. Current opinion in plant biology **13**, 273-278.

Smotrys JE, Schoenfish MJ, Stutz MA, Linder ME. 2005. The vacuolar DHHC-CRD protein Pfa3p is a protein acyltransferase for Vac8p. The Journal of cell biology **170**, 1091-1099.

Swarthout JT, Lobo S, Farh L, Croke MR, Greentree WK, Deschenes RJ, Linder ME. 2005. DHHC9 and GCP16 constitute a human protein fatty acyltransferase with specificity for H-and N-Ras. Journal of Biological Chemistry **280**, 31141-31148.

Thazar-Poulot N, Miquel M, Fobis-Loisy I, Gaude T. 2015. Peroxisome extensions deliver the Arabidopsis SDP1 lipase to oil bodies. Proceedings of the National Academy of Sciences **112**, 4158-4163.

Theodoulou FL, Eastmond PJ. 2012. Seed storage oil catabolism: a story of give and take. Current opinion in plant biology **15**, 322-328.

Valdez- Taubas J, Pelham H. 2005. Swf1- dependent palmitoylation of the SNARE Tlg1 prevents its ubiquitination and degradation. The EMBO journal **24**, 2524-2532.

Vetrivel KS, Meckler X, Chen Y, Nguyen PD, Seidah NG, Vassar R, Wong PC, Fukata M, Kounnas MZ, Thinakaran G. 2009. Alzheimer disease Aβ production in the absence of S-palmitoylation-dependent targeting of BACE1 to lipid rafts. Journal of Biological Chemistry **284**, 3793-3803.

Yeste-Velasco M, Linder ME, Lu Y-J. 2015. Protein S-palmitoylation and cancer. Biochimica et Biophysica Acta (BBA)-Reviews on Cancer **1856**, 107-120.

Yuan X, Zhang S, Sun M, Liu S, Qi B, Li X. 2013. Putative DHHC-Cysteine-Rich Domain S-Acyltransferase in Plants. PloS ONE **8**.

Zhao L, Lobo S, Dong X, Ault AD, Deschenes RJ. 2002. Erf4p and Erf2p form an endoplasmic reticulum-associated complex involved in the plasma membrane localization of yeast Ras proteins. Journal of Biological Chemistry **277**, 49352-49359.

Zhao M, Zhang H, Yan H, Qiu L and Baskin CC. 2018. Mobilization and role of starch, protein, and fat reserves during seed germination of six wild grassland species. Frontiers in Plant Science. **9**, 234. doi: 10.3389/fpls.2018.00234

Zolman BK, Martinez N, Millius A, Adham AR, Bartel B. 2008. Identification and characterization of Arabidopsis indole-3-butyric acid response mutants defective in novel peroxisomal enzymes. Genetics **180**, 237-251.

Zolman BK, Silva ID, Bartel B. 2001. The Arabidopsis pxa1 mutant is defective in an ATP-binding cassette transporter-like protein required for peroxisomal fatty acid β-oxidation. Plant Physiology **127**, 1266-1278.

Figure legends

Fig 1. Characterization of the Arabidopsis SALK T-DNA homozygous mutant insertion line for *AtPAT15*.

(A) Schematic structure of the *PAT15* gene and position of the T-DNA insertion in SALK_006515. Solid boxes represent exons, empty boxes untranslated regions and lines introns.

(B) RT-PCR with different primer pairs to show that the *pat15-1* mutant is devoid of the transcripts spanning the T-DNA insertion site (F139+R981, F564+R910) although transcripts upstream (F139+R453) and downstream (F813+R1045) were detected. Positions of the primers are indicated in A.

(A) &(D) 1-week (C) and 4-week (D) old WT and *pat15-1* plants. Arrow in C indicates curled cotyledon and arrowhead the smaller meristems of *atpat15-1*. Arrow in D indicates small abnormal meristem in *atpat15-1*.

(E) Rosette leaves of WT and *pat15-1* plants taken from 26-day-old plants.

(F) Morphology of mature seeds from WT and *pat15-1* plants.

(G) Dry weight per seed of WT and *pat15-1*. The experiment was repeated five times using approximately 100 seeds in each replicate. * $p<0.05$ in Student's *t*-test.

Fig 2. The temporal and spatial expression of *PAT15* in seedlings and different tissues of the mature plant of Arabidopsis.

(A) RT-PCR was carried out on total RNA isolated from WT Col-0 whole seedlings and different parts of the mature plants. Se, 7-day-old seedlings grown on ½ MS media; R, roots of 2-week-old seedlings grown on ½ MS media; St, stem of the first node of 35-day-old soil-grown plants; L, the 5th and 6th rosette leaves of 4-week-old soil-grown plants; F, fully-opened flowers; Si, 3-day-old siliques after pollination. *GAPC* was used as loading control.

(B) Histochemical localization of PAT15. A construct containing PAT15promoter:GUS fusion was transformed to WT Arabidopsis plants. GUS-staining was performed on whole seedlings and different tissues of the mature transgenic plants. a, 1-week-old seedlings; b, 2-week-old seedlings; c, the fully expended rosette leaf of 5-week-old plant; d&e, inflorescence and flower from 5-week-old plants.

Fig 3. AtPAT15 is an *S*-acyltransferase.

(A) AtPAT15 partially rescues the growth defect of *akr1*. Yeast cells of all 4 genotypes were cultured in the induction media at 37ºC and observed by DIC light microscopy. Cells were transformed with empty vector pYES2 (WT and *akr1*), or with AtPAT15 and AtPAT15C^{122}S (*akr1*-PAT15, *akr1*-PAT15C^{122}S). Arrows indicate elongated cells. Scale bar = 10 µm.

(B) AtPAT15 is auto-acylated. The Acyl-RAC assay was carried out on total proteins extracted from transgenic *akr1* yeast cells expressing AtPAT15 and AtPAT15C^{122}S and detected by Western blotting with anti-V5 antibody using the ECL method. The molecular weight of AtPAT15 and AtPAT15C^{122}S is ~ 30.6 kDa. A band corresponding to AtPAT15-V5 was detected in the + NH_2OH treated sample, indicating that it is bound to an acyl group via a labile thioester linkage confirming that it is auto-acylated. However, no signal was detected for AtPAT15C^{122}S indicating that it is not auto-acylated. LC: loading control, lanes +: NH_2OH treated and lanes -: non NH_2OH treated.

Fig 4. PAT15 is targeted to the Golgi.

AtPAT15-GFP or AtPAT15C^{122}S-GFP were co-expressed with AtGNT1-mCherry transiently in Arabidopsis seedlings. Localization of the florescent proteins were observed by laser scanning confocal microscopy. Bars = 15 µm.

Fig 5. Both PAT15 and PAT15DHHC^{122}S can rescue the growth defect of *pat15-1*. 3-week-old plants are shown.

Fig 6. Defects in seed germination and early seedling growth of *pat15-1*.

(A) Seed germination of *pat15-1* is slower than WT. Germination rate of WT and *pat15-1* after 16-, 24-, 48- and 72 hours on ½ MS media without 1% sucrose. * $p<0.05$ in Student's *t*-test.

(B) Early seedling growth of *pat15-1* is sugar dependent. Seedlings were vertically cultured on ½ MS media for 7 days without (left) or with (right) 1% sucrose.

Fig 7. *pat15-1* has defect in lipid breakdown during post-germination growth.

(A) Content of C20:1 in seeds and dark-grown seedlings. Total fatty acids were extracted from seeds or 5-day-old etiolated seedlings of WT, *pat15-1* and *sdp1* that were grown on ½ MS without (-SUC) or with 1% sucrose (+SUC). The content of C20:1, a marker for TAG, was analyzed by GC-MS. The values are the means±SE of measurements from four separate batches of 30 seeds or 40 seedlings. Different letters above the columns indicate statistically different values analyzed by one-way ANOVA and post hoc test.

(B) Observation of oil droplets in the hypocotyls of WT and *pat15-1* seedlings. 5-day-old etiolated seedlings were stained with Nile Red and the hypocotyls were observed under DIC light microscopy (left), or confocal laser scanning microscopy (right). Bars = 0.1mm.

Fig 8. Transcript levels of the key genes involved in lipid breakdown pathway were down-regulated during early seedling growth. Total RNA was extracted from 10 seedlings of WT or *pat15-1* that were grown on ½ MS+1% Suc for 10 days in the dark. The relative expression level of each gene in the mutant was calculated where the transcript level of WT was regarded as 1. The experiments were repeated three times. * $p<0.05$ in Student's *t*-test. *KAT2, 3-ketoacyl-CoA thiolase 2; ICL, isocitrate lyase; MLS, malate synthase; PCK1, phosphoenolpyruvate carboxykinase1*.

Fig 9. β-oxidation process is disrupted in the loss-of-function of PAT15 mutant.
(A) Effect of 2, 4-D and 2, 4-DB on root growth. Both WT and *pat15-1* seedlings were grown on agar plates containing ½ MS+1% sucrose (control), or supplemented with 0.5 µM 2, 4-DB or 2, 4-D as indicated. The seedlings were grown under LD conditions for 7 days.

(B) Root lengths of seedlings from A. 20 seedlings were measured. * $p<0.01$ in Student's *t*-test.

(C) Effect of 2, 4-D and 2, 4-DB on hypocotyl length. Both WT and *pat15-1* seedlings were grown in the dark for 4 days on ½ MS (control), or media supplemented with 1µM 2, 4-D or 2, 4-DB.

(D) Hypocotyl length. The hypocotyl lengths of at least 30 seedlings of each line shown in (C) were measured. Different letters above the columns indicate statistically different values analyzed by one-way ANOVA and Tukey's HSD test.
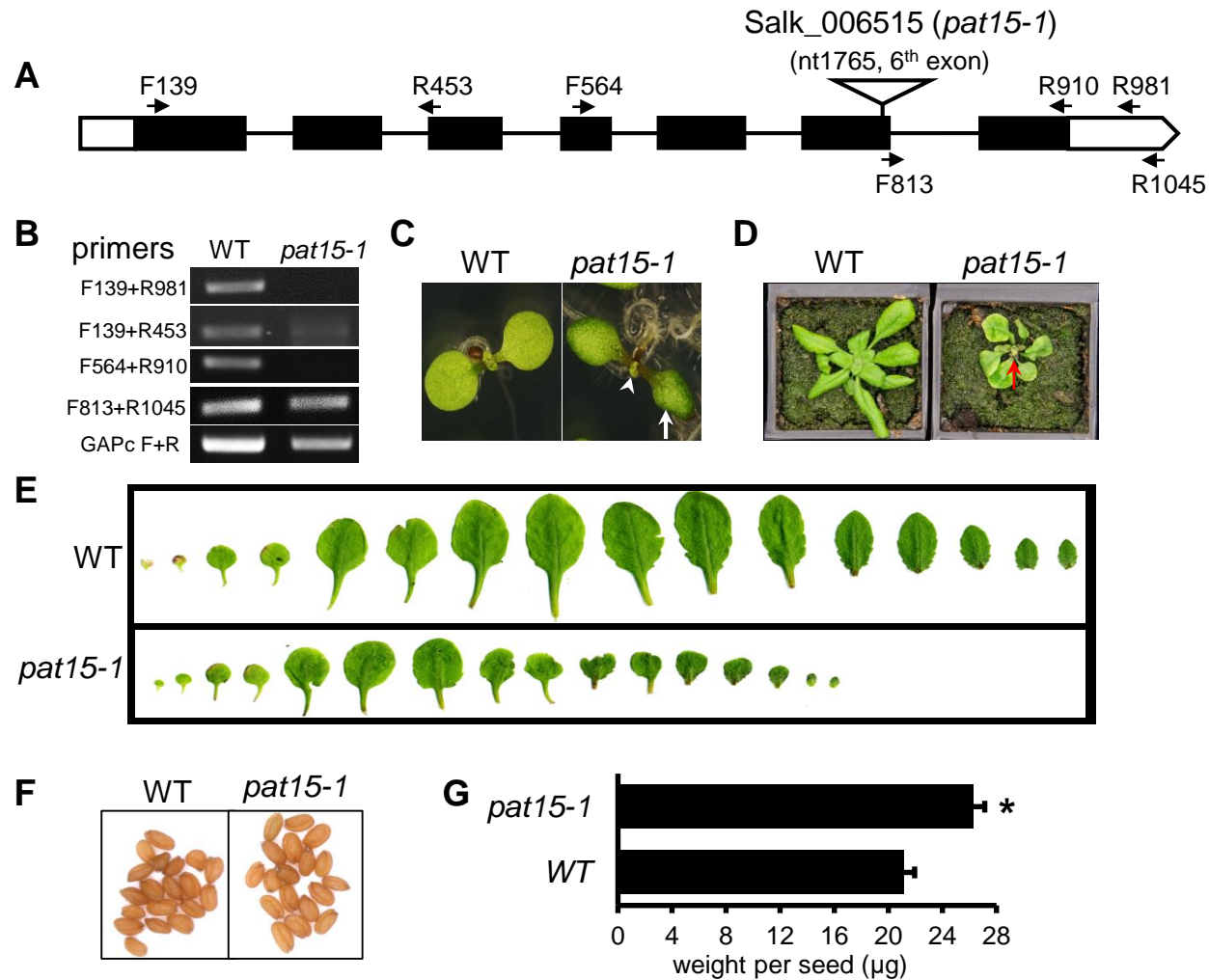
Table 1. Phenotypic analysis of WT and *pat15-1*

	WT (n=9)	*pat15-1* (n=10)
Plant height (mm)	476.0±18.9	420.9±10.1*
Length of silique (mm)	17.0±0.7	16.3±1.1
No. of branches	23.0±2.8	20.1±3.2
No. of siliques in main branch	55.8±1.9	45.4±3.8*

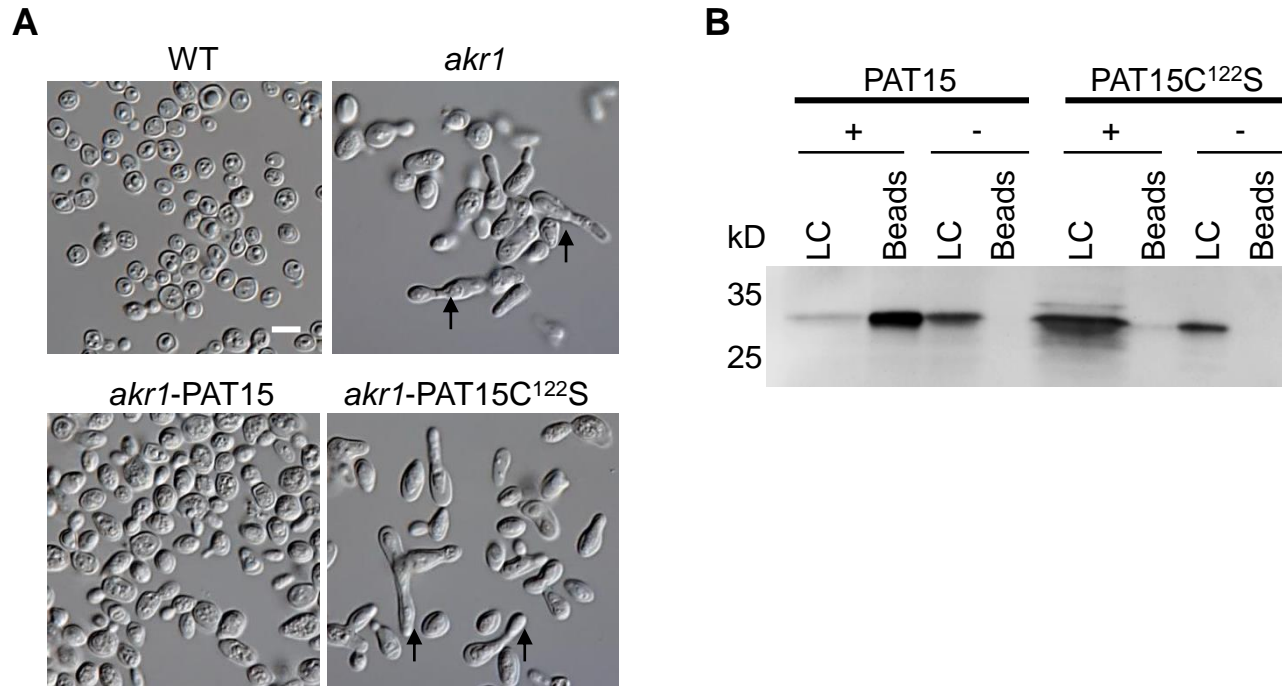62-day-old plants were analysed. *$p<0.01$ in Student's *t*-test.

Fig. 1. Characterization of the Arabidopsis SALK T-DNA homozygous mutant insertion line for *AtPAT15*.

(A) Schematic structure of the *PAT15* gene and position of the T-DNA insertion in SALK_006515. Solid boxes represent exons, empty boxes untranslated regions and lines introns.

(B) RT-PCR with different primer pairs to show that the *pat15-1* mutant is devoid of the transcripts spanning the T-DNA insertion site (F139+R981, F564+R910) although transcripts upstream (F139+R453) and downstream (F813+R1045) were detected. Positions of the primers are indicated in A.

(C) &(D) 1-week (C) and 4-week (D) old WT and *pat15-1* plants. Arrow in C indicates curled cotyledon and arrowhead the smaller meristems of *atpat15-1*. Arrow in D indicates small abnormal meristem in *atpat15-1*.

(E) Rosette leaves of WT and *pat15-1* plants taken from 26-day-old plants.

(F) Morphology of mature seeds from WT and *pat15-1* plants.

(G) Dry weight per seed of WT and *pat15-1*. The experiment was repeated five times using approximately 100 seeds in each replicate. * $p<0.05$ in Student's *t*-test.

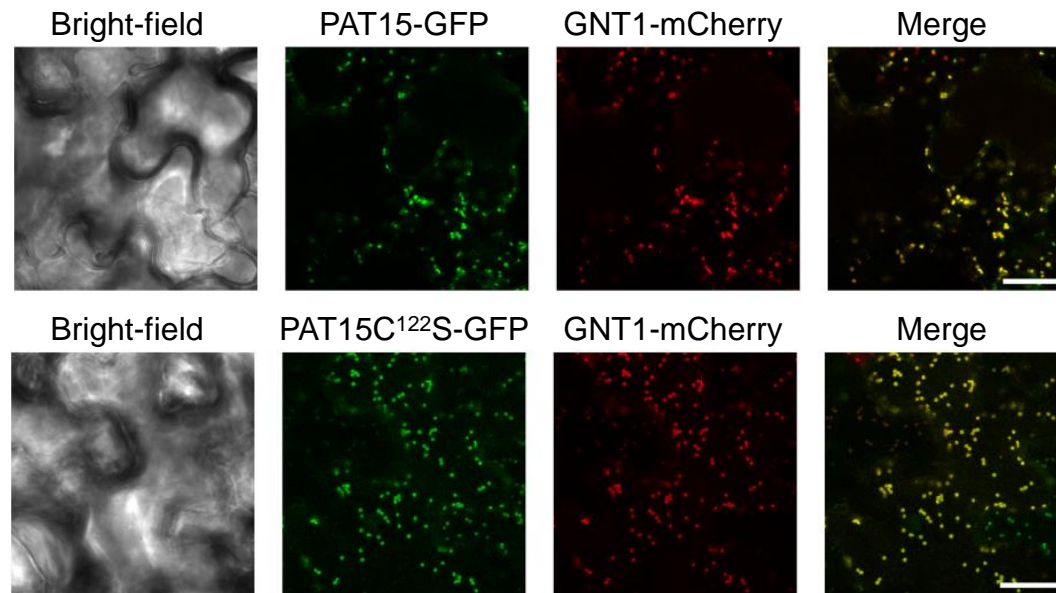**A**

B

Fig. 2. The temporal and spatial expression of *PAT15* in seedlings and different tissues of the mature plant of Arabidopsis.

(A) RT-PCR was carried out on total RNA isolated from WT Col-0 whole seedlings and different parts of the mature plants. Se, 7-day-old seedlings grown on ½ MS media; R, roots of 2-week-old seedlings grown on ½ MS media; St, stem of the first node of 35-day-old soil-grown plants; L, the 5th and 6th rosette leaves of 4-week-old soil-grown plants; F, fully-opened flowers; Si, 3-day-old siliques after pollination. *GAPC* was used as loading control.

(B) Histochemical localization of PAT15. A construct containing PAT15promoter:GUS fusion was transformed to WT Arabidopsis plants. GUS-staining was performed on whole seedlings and different tissues of the mature transgenic plants. a, 1-week-old seedlings; b, 2-week-old seedlings; c, the fully expended rosette leaf of 5-week-old plant; d&e, inflorescence and flower from 5-week-old plants.
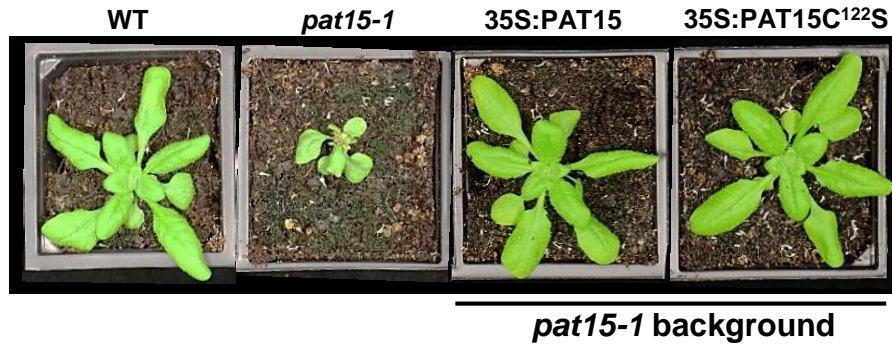
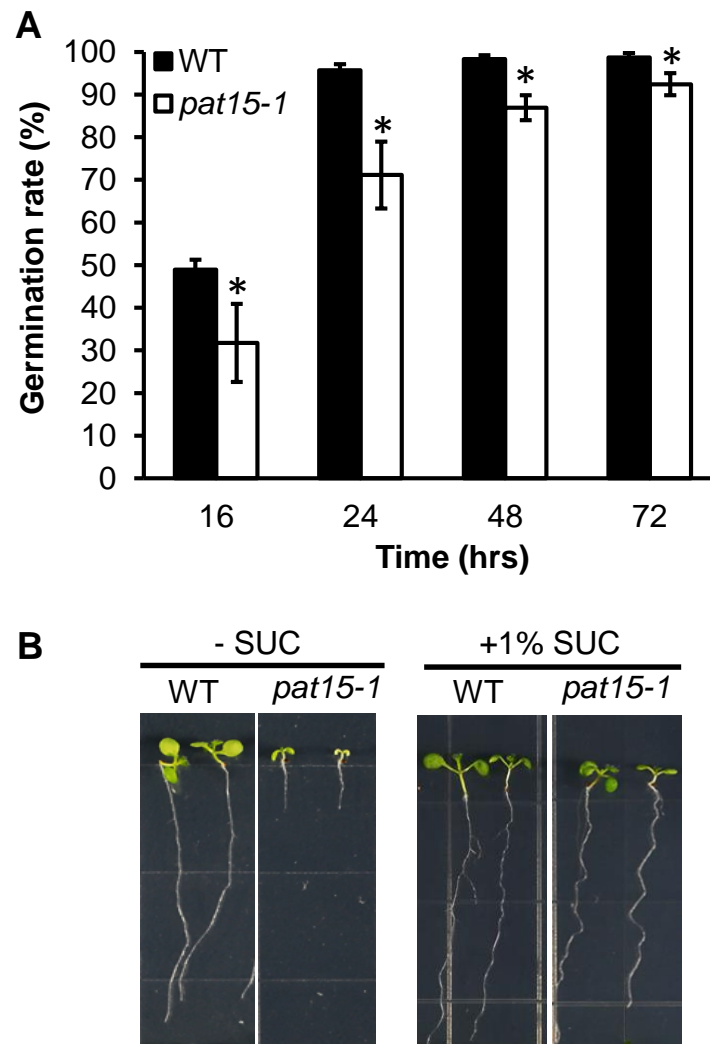**Fig 3.** AtPAT15 is an *S*-acyltransferase.

(A) AtPAT15 partially rescues the growth defect of *akr1*. Yeast cells of all 4 genotypes were cultured in the induction media at 37ºC and observed by DIC light microscopy. Cells were transformed with empty vector pYES2 (WT and *akr1*), or with AtPAT15 and AtPAT15C^{122}S (*akr1*-PAT15, *akr1*-PAT15C^{122}S). Arrows indicate elongated cells. Scale bar = 10 µm.

(B) AtPAT15 is auto-acylated. The Acyl-RAC assay was carried out on total proteins extracted from transgenic *akr1* yeast cells expressing AtPAT15 and AtPAT15C^{122}S and detected by Western blotting with anti-V5 antibody using the ECL method. The molecular weight of AtPAT15 and AtPAT15C^{122}S is ~ 30.6 kDa. A band corresponding to AtPAT15-V5 was detected in the + NH$_2$OH treated sample, indicating that it is bound to an acyl group via a labile thioester linkage confirming that it is auto-acylated. However, no signal was detected for AtPAT15C^{122}S indicating that it is not auto-acylated. LC: loading control, lanes +: NH$_2$OH treated and lanes -: non NH$_2$OH treated.

Bright-field	PAT15-GFP	GNT1-mCherry	Merge

Bright-field	PAT15C^{122}S-GFP	GNT1-mCherry	Merge

Fig 4. PAT15 is targeted to the Golgi.
AtPAT15-GFP or AtPAT15C^{122}S-GFP were co-expressed with AtGNT1-mCherry transiently in Arabidopsis seedlings. Localization of the florescent proteins were observed by laser scanning confocal microscopy. Bars = 15 µm.
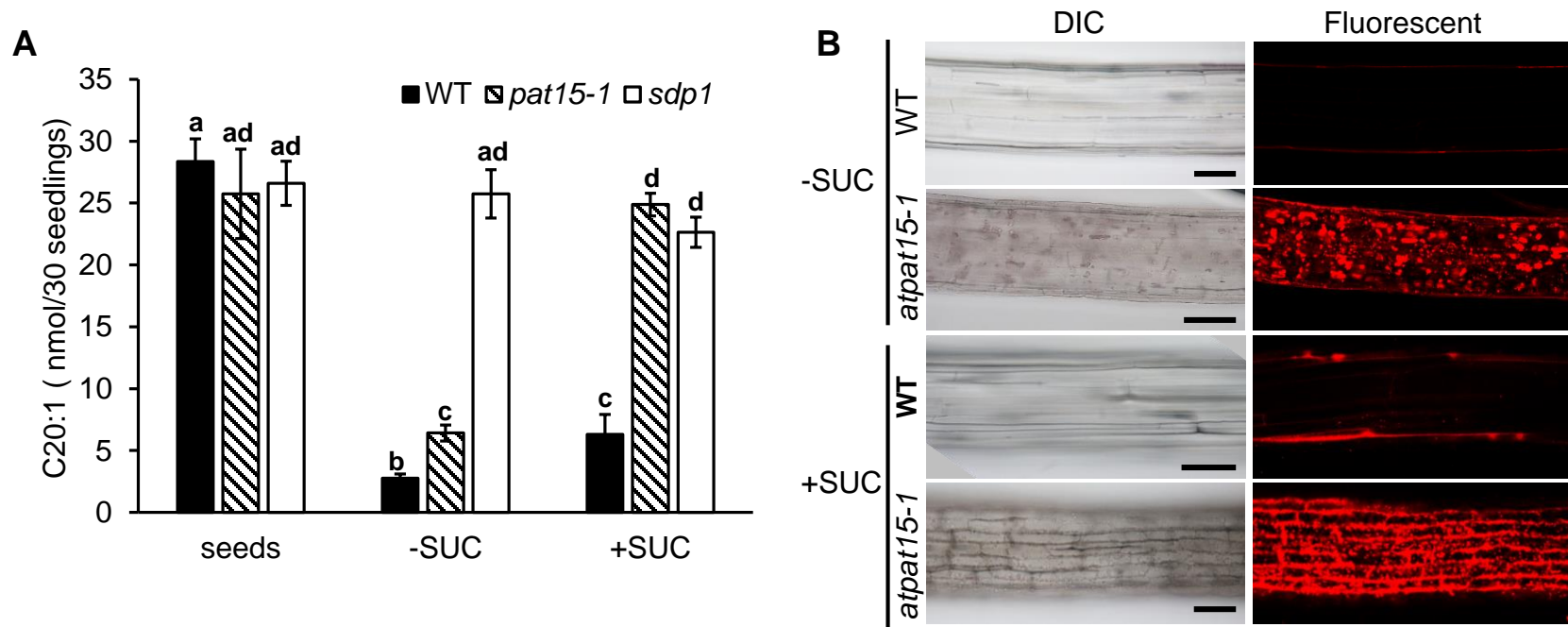
Fig 5. Both PAT15 and PAT15DHHC^{122}S can rescue the growth defect of *pat15-1*. Three-week-old plants are shown.

Fig 6. Defects in seed germination and early seedling growth of *pat15-1*.

(A) Seed germination of *pat15-1* is slower than WT. Germination rate of WT and *pat15-1* after 16-, 24-, 48- and 72 hours on ½ MS media without 1% sucrose. * *p*<0.05 in Student's *t*-test.

(B) Early seedling growth of *pat15-1* is sugar dependent. Seedlings were vertically cultured on ½ MS media for 7 days without (left) or with (right) 1% sucrose.
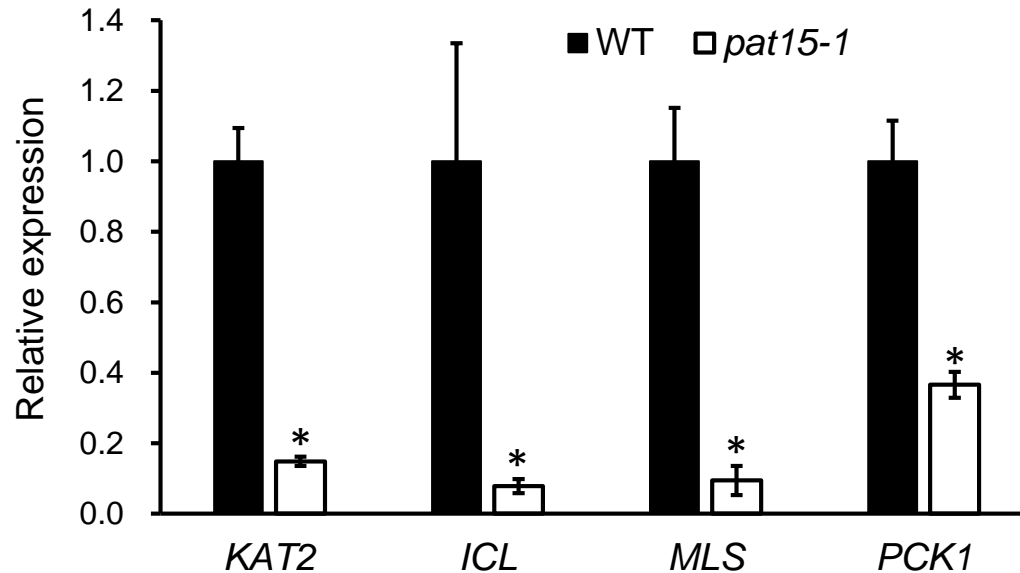
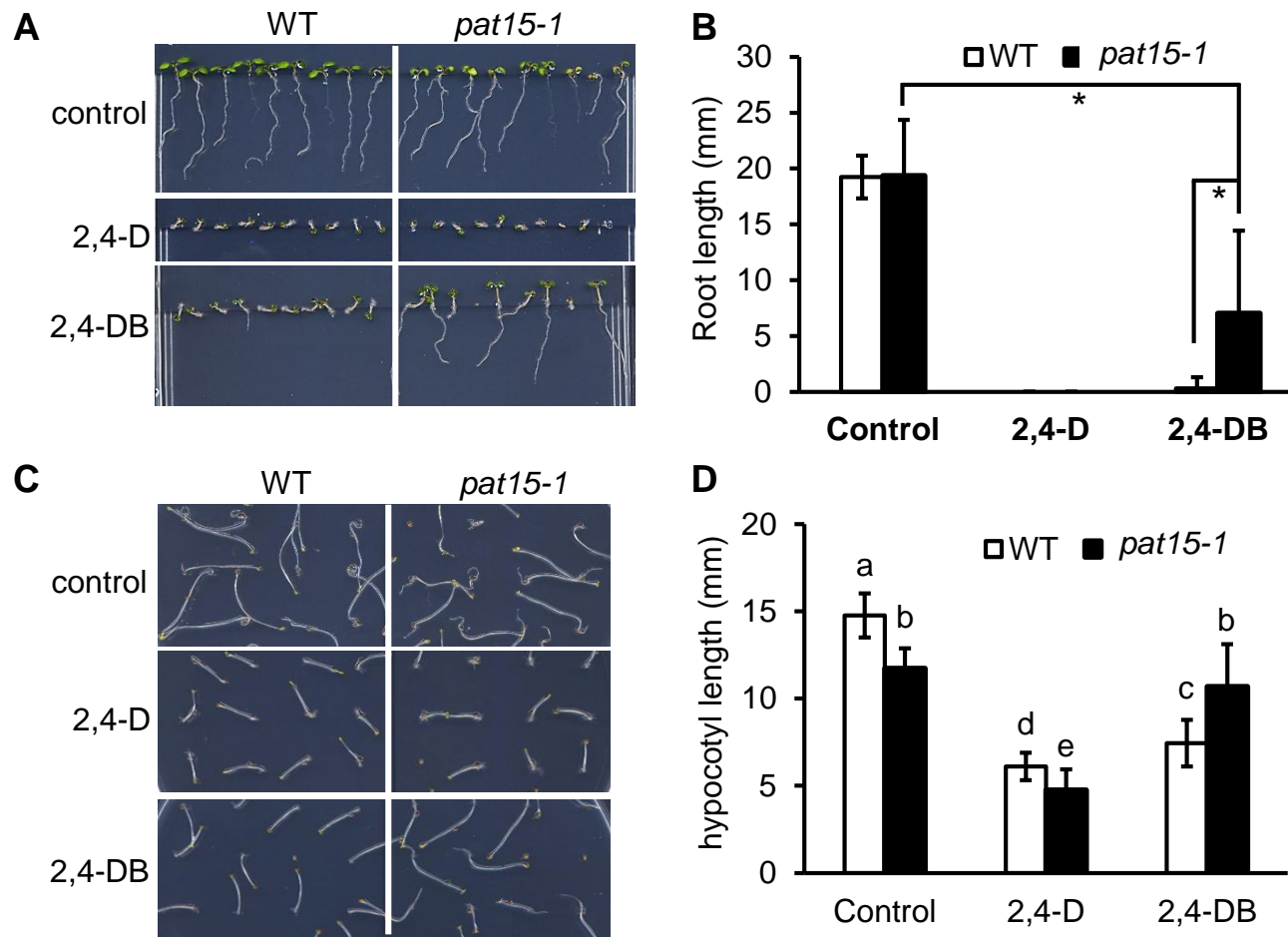**Fig. 7**. *pat15-1* has defect in lipid breakdown during post-germination growth.

(A) Content of C20:1 in seeds and dark-grown seedlings. Total fatty acids were extracted from seeds or 5-day-old etiolated seedlings of WT, *pat15-1* and *sdp1* that were grown on ½ MS without (-SUC) or with 1% sucrose (+SUC). The content of C20:1, a marker for TAG, was analysed by GC-MS. The values are the means $\pm$ SE of measurements from four separate batches of 30 seeds or 40 seedlings. Different letters above the columns indicate statistically different values analyzed by one-way ANOVA and post hoc test.

(B) Observation of oil droplets in the hypocotyls of WT and *pat15-1* seedlings. 5-day-old etiolated seedlings were stained with Nile Red and the hypocotyls were observed under DIC light microscopy (left), or confocal laser scanning microscopy (right). Bars = 0.1mm.

Fig. 8. Transcript levels of the key genes involved in lipid breakdown pathway were down-regulated during early seedling growth. Total RNA was extracted from 10 seedlings of WT or *pat15-1* that were grown on ½ MS+1% Suc for 10 days in the dark. The relative expression level of each gene in the mutant was calculated where the transcript level of WT was regarded as 1. The experiments were repeated three times. * *p*<0.05 in Student's *t*-test. *KAT2, 3-ketoacyl-CoA thiolase 2; ICL, isocitrate lyase; MLS, malate synthase; PCK1, phosphoenolpyruvate carboxykinase1*.

Fig 9. β-oxidation process is disrupted in the loss-of-function of PAT15 mutant.

(A) Effect of 2, 4-D and 2, 4-DB on root growth. Both WT and *pat15-1* seedlings were grown on agar plates containing ½ MS+1% sucrose (control), or supplemented with 0.5 µM 2, 4-DB or 2, 4-D as indicated. The seedlings were grown under LD conditions for 7 days.

(B) Root lengths of seedlings from A. 20 seedlings were measured. * *p*<0.01 in Student's *t*-test.

(C) Effect of 2, 4-D and 2, 4-DB on hypocotyl length. Both WT and *pat15-1* seedlings were grown in the dark for 4 days on ½ MS (control), or media supplemented with 1µM 2, 4-D or 2, 4-DB.

(D) Hypocotyl length. The hypocotyl lengths of at least 30 seedlings of each line shown in (C) were measured. Different letters above the columns indicate statistically different values analyzed by one-way ANOVA and Tukey's HSD test.